Infrared Physics and Technology 93 (2018) 70–76

Contents lists available at ScienceDirect

Infrared Physics & Technology

journal homepage: www.elsevier.com/locate/infrared

Regular article

Analysis injection area-dark current characteristics for mid-wavelength HgCdTe photodiodes

W.K. Zhang[a,b], J.M. Lin[a], H.L. Chen[a], H. Li[a], R. Wang[c], R.J. Ding[a,*]

[a] Key Laboratory of Infrared Imaging Materials and Detectors, Shanghai Institute of Technical Physics, Chinese Academy of Sciences, Shanghai 200083, China
[b] University of Chinese Academy of Science, Beijing 100049, China
[c] College of Advanced Interdisciplinary Studies, National University of Defense Technology, Changsha 410073, China

ARTICLE INFO

Keywords:
HgCdTe
Dark current
Injection area
Reverse welding pressure
Arrangement of common electrode

ABSTRACT

In this paper, we study the relationship between dark current mechanism and the injection area of mid-wavelength infrared (MWIR) HgCdTe photovoltaic detectors. A simultaneous-mode nonlinear fitting program for n-on-p mid-wavelength HgCdTe infrared detectors is reported. It is found that the impact of diffusion mechanism gradually weakens and the effect of generation-recombination mechanism becomes more significant as the area of injection increasing under forward bias. The effect of trap-assisted tunneling mechanism gradually weakens as the area of injection increasing under middle reverse bias and band-to-band tunneling mechanism has less impact on dark current of MWIR HgCdTe photodiodes. And as the area of injection increasing, the effect of surface leak mechanism is gradually decrease. Finally, we find the reversed welding pressure and the arrangement of common electrode for MWIR HgCdTe Photodiodes also impacts diffusion mechanism and generation-recombination mechanism under forward bias.

1. Introduction

$Hg_{1-x}Cd_xTe$ (Mercury Cadmium Telluride, MCT) photodiodes have always been one of the high-performance infrared detectors because of high electron mobility, high quantum efficiency and adjustable bandgap [1,2]. The dark current restricts the performance of the MCT infrared detector that affects the noise and quantum efficiency of the device. The dark current also directly affects the detection distance of target which makes the false alarm of the infrared detection system. It can provide references for process optimization to reduce the dark current of MCT infrared detectors by analyzing dark current mechanisms [3,4]. The dark current mechanism is mainly related to substrate material defects and the process of MCT photodiodes. It can be modeled with a combination of diffusion current (I_{diff}), generation-recombination current (I_{gr}), trap-assisted tunneling current (I_{tat}), and band-to-band tunneling current (I_{bbt}) [5]. There are multiple dark current mechanisms dominated at most bias voltages for dark current of the MCT infrared detector. The non-parabolic conduction band and the effects of carrier degeneracy has great impact on the MCT device model simulation. Z.J. Quan builds the new MCT device model which takes account of carrier degeneracy and conduction band non-parabolicity to analyze characteristics of long-wavelength MCT n-on-p photodiodes [6–8]. The non-uniformity is a major issue in large area IR detector arrays of HgCdTe. R.S. Saxena presents the effect of variations in the various device and material parameters on the performance of MWIR MCT photodiodes [9]. Temperature also has great impact on the dominant of dark current mechanism [10,11]. The area of injection impacts the contact of PN junction and affects electron mobility which influence the width and electric field of space charge region. Therefore, it is great significance to study the relationship between the area of injection and the components of dark current mechanism.

In this paper, we research the relationship between the area of injection and dark current mechanism of the MWIR HgCdTe photodiodes by new MCT device fitting-model using the R-V curves measured. By studying the p-V curves, it is found that the slope of p-V curve near the zero-bias decreases for DIFF mechanism and the slope of p-V curves has great variation for GR mechanism under small reverse bias. And we find that it is caused by the reversed welding pressure and arrangement of common electrode for MWIR HgCdTe photodiodes.

2. Theoretical models

The dark current mechanism of MCT photodiodes is modeled with the combination of diffusion (DIFF) current, generation-recombination (GR) current, trap-assisted- tunneling (TAT) current, and band-to-band tunneling (BBT) current. The surface leakage currents and the

---

* Corresponding author.
E-mail addresses: zhangwukang14@mails.ucas.ac.cn (W.K. Zhang), dingrj@mail.sitp.ac.cn (R.J. Ding).

https://doi.org/10.1016/j.infrared.2018.07.010
Received 14 May 2018; Received in revised form 9 July 2018; Accepted 10 July 2018

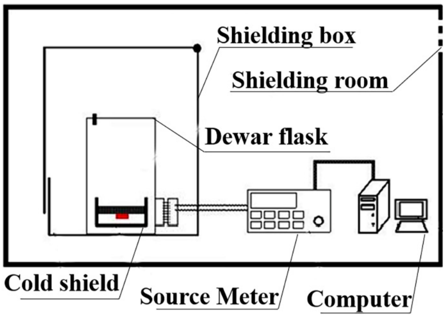

Fig. 1. MCT infrared detector I-V test platform.

Table 1
Material and device parameters of I–VI photovoltaic samples.

Sample number	I	II	III	IV	V	VI
x	0.3049	0.3033	0.3048	0.3034	0.2986	0.3007
$A \times 10^{-5}$ (cm^2)	10.0	40.0	78.4	96.0	78.4	40.0
$N_a \times 10^{15}$ (cm^{-3})	6.63	6.01	8.91	9.01	6.75	6.48
μ_p (cm$^2/V_s$)	441.9	363.5	466.9	451.3	554.2	477
f (kg/s)	2.5	2.5	2.0	1.5	1.7	2.5

dislocations in the material, which intersect the junction, are generally held responsible as a possible source of ohmic current. Taking series resistance R_s into account, the total resistance R_{exp} generated by the measured dark current can be expressed as [6,7,12]:

$$R_{exp} = \left(\frac{1}{R_{diff}} + \frac{1}{R_{gr}} + \frac{1}{R_{tat}} + \frac{1}{R_{bbt}} + \frac{1}{R_{shunt}}\right)^{-1} + R_s \tag{1}$$

R_{diff}, R_{gr}, R_{tat}, R_{bbt} respectively indicates the corresponding resistance generated by the four mechanisms of dark current. R_{shunt} is the diodes shunt resistance. The resistance R_{diff} generated by diffusion current is given as [13–15]:

$$R_{diff} = \left(\frac{dI_{diff}}{dV_e}\right)^{-1} = \left[AJ_{diff0}\frac{q}{kt}\exp\left(\frac{qv}{kt}\right)\right]^{-1} \tag{2}$$

J_{diff0} is given as:

$$J_{diff0} = qn_i^2\sqrt{\frac{kt}{q}}\left(\sqrt{\frac{\mu_n}{\tau_n}}\frac{1}{N_a} + \sqrt{\frac{\mu_p}{\tau_p}}\frac{1}{N_d}\right) \tag{3}$$

Here A is the area of injection; n_i is the intrinsic carrier concentration; μ_n and μ_p represent the electron and hole mobility respectively; τ_p and τ_n represent the lifetime of minority carriers in the n and p region; N_a and N_d represent the dopant density in the p and n region respectively; q is the quantity of electric charge; k and T represent the Boltzmann constant and the temperature respectively; The bias voltage is an effective bias $R_e = V{-}IR_s$ corrected by the series resistance R_s. Here, V is the applied voltage and I is the total dark current.

The resistance R_{gr} generated by generation-recombination current is given as [13,16]:

$$R_{gr} = \left(\frac{dI_{gr}}{dV_e}\right)^{-1} = \frac{\tau_0\sqrt{V_{bi}}}{A2n_iw_0kT}\left[\frac{\cosh\left(\frac{qV}{2kT}\right)\frac{qV}{2kT}f(b) + \sinh\left(\frac{qV}{2kT}\right)\frac{df(b)}{dV}}{\sqrt{V_{bi}-V}} + \frac{\sinh\left(\frac{qV}{2kT}\right)f(b)}{2(V_{bi}-V)^{\frac{3}{2}}}\right]^{-1} \tag{4}$$

Here τ_0 and W_0 respectively represent the effective lifetime in the depletion region and the width of the depletion region under the zero bias; V_{bi} is the build-up potential inside PN junction. $f(b)$ can be expressed as:

$$f(b) = \begin{cases} \frac{\ln(b + \sqrt{b^2 - 1})}{\sqrt{b^2 - 1}} & b > 1 \\ \frac{1}{b} & b = 1 \\ \frac{1}{\sqrt{1 - b^2}}\left[\frac{\pi}{2} - \arctan\left(\frac{b}{\sqrt{1 - b^2}}\right)\right] & b < 1 \end{cases} \tag{5}$$

b is given as:

$$b = \exp\left(\frac{-qV}{2kT}\right)\cosh\left[\frac{E_t - E_i}{kT} + \frac{1}{2}\ln\left(\frac{\tau_p}{\tau_n}\right)\right] \tag{6}$$

here E_t and E_i represent the trap energy level and the intrinsic Fermi energy level respectively.

The resistance R_{bbt} generated by band-to-band tunneling current is given as [13,17]:

$$R_{bbt} = \left(\frac{dI_{bbt}}{dV_e}\right)^{-1} = \left[bbt_1(-1.5\sqrt{V_{bi} - V} + 0.5)\exp\left(\frac{bbt_2}{\sqrt{V_{bi} - V}}\right)\right]^{-1} \tag{7}$$

bbt_1 can be expressed as:

$$bbt_1 = -A\frac{q^3\sqrt{2m_e}}{4\pi^3\hbar^2\sqrt{E_g}}\sqrt{\frac{qN_aN_d}{2\varepsilon_s\varepsilon_0(N_a + N_d)}} \tag{8}$$

bbt_2 can be expressed as:

$$bbt_2 = -\frac{\pi\sqrt{\frac{m_e}{2}}E_g^{\frac{3}{2}}}{2q\hbar}\sqrt{\frac{2\varepsilon_s\varepsilon_0(N_a + N_d)}{qN_aN_d}} \tag{9}$$

Here m_e and E_g represent the electron effective mass and the band gap respectively;

The resistance R_{tat} generated by trap-assisted tunneling current is given as [13,18,19]:

$$R_{tat} = \left(\frac{dI_{tat}}{dV_e}\right)^{-1} = \left[-tat_1\exp\left(\frac{tat_2}{\sqrt{V_{bi} - V}}\right)\left(1 - \frac{tat_2}{2\sqrt{V_{bi} - V}}\right)\right]^{-1} \tag{10}$$

The tat_1 can be expressed as:

$$tat_1 = -\frac{A\pi^2q^2N_tm_eM^2}{h^3(E_g - E_t)} \tag{11}$$

And tat_2 can be expressed as:

$$tat_2 = -\frac{\sqrt{3}E_g^3F(a)}{8\sqrt{2qP}}\sqrt{\frac{2\varepsilon_s\varepsilon_0(N_a + N_d)}{qN_aN_d}} \tag{12}$$

The $F(a)$ is given as:

$$F(a) = \frac{\pi}{2}\sin^{-1}(1 - 2a) + 2(1 - 2a)\sqrt{a(1 - a)},\ a = \frac{E_t}{E_g} \tag{13}$$

Here M and P represent the transition matrix element and Kane matrix element respectively. The N_t represents defect concentration in the depleted region.

The diodes shunt resistance R_{shunt} generated by excess current component is given as:

$$R_{shunt} = \frac{V_e}{I_{sh}} \tag{14}$$

Here the I_{sh} is an Ohmic current. The surface leakage currents and the dislocations in the material that intersect the junction are generally held responsible as a possible source for this part of excess current. For the diodes with small leakage current, the highest value of dynamic resistance may be assumed as the shunt resistance of the diode.